Open Access Online Journal on Astronomy and Astrophysics
Acta Astrophysica Taurica
www.astrophysicataurica.org

Acta Astrophys. Tau. 7(3), 1–4 (2026) EDN: HZKBKR

Technique for processing the RATAN-600 sky survey at the declination of the Crab Nebula

N.N. Bursov, A.A. Kudryashova

Special Astrophysical Observatory, Nizhnij Arkhyz 369167, Zelenchukskiy region, Karachai-Cherkessian Republic, Russian Federation
e-mail: nnb@sao.ru

Received 15 November 2023

ABSTRACT

In this paper we present the results of developing a method for processing the sky survey obtained with the fixed antenna of the RATAN-600 Western Sector ($Az = 270°$) at the declination of the pulsar in the Crab Nebula. The sky survey was conducted in 2018–2019 using a complex of three four-channel radiometers at a central frequency of 4.7 GHz. We consider the peculiarities of the passage of sources at a parallactic angle through the antenna beam pattern, with input horns of radiometers located along the focal line of the secondary mirror. A sample of 205 sources with $S/N > 50$ ($S_{4.7} > 15$ mJy) was processed. For the detected and identified sources, we calculated ephemerides for the observational epoch, depending on their offset relative to the telescope beam pattern centers in each receiving horn of the radiometers. During data accumulation, the measured positions of the sources were corrected, and a change in the gain of the radiometers due to ambient temperature was taken into account. The proposed method allows one to determine both the position of the detected sources with an accuracy of 1–2 seconds and flux densities with an accuracy of 5–10%.

Key words: radio telescope, observations, data analysis, data processing methods

1 Introduction

Sky surveys are the traditional observation method in radio astronomy. Surveys reveal objects that subsequently become the subjects of comprehensive studies. The first radio survey in the USSR was carried out at the Crimean Astrophysical Observatory in 1969 using the RT-22 radio telescope at a wavelength of 3 cm, with an expected source detection threshold exceeding 1 Jy. The Sternberg Astronomical Institute of Moscow State University (SAI MSU) and the V.I. Lenin Moscow State Pedagogical Institute took part in both its preparation and development of a hardware and software complex (Volvach, Larionov, 2008). The first deep survey at the declination of the source SS 433 was carried out with the RATAN-600 radio telescope in 1981 at a wavelength of 7.6 cm, achieving a record flux density sensitivity $S_{3.9} < 7.5$ mJy (Pariiski et al., 1991). Since 2017, round-the-clock sky surveys at various declinations have been conducted with the RATAN-600 Western Sector using a complex of three to four four-channel radiometers at a central frequency of 4.7 GHz (Bursov et al., 2022).

RATAN-600 is a transit telescope; it allows one to perform measurements of the antenna temperature depending on the sidereal time during the passage across the sky through the stationary beam pattern (BP) of the telescope due to the Earth's rotation. Observations are carried out in the eastward direction, where sources are rising. An important characteristic is that sources in each survey pass through the BP at different angles relative to its central cross-section. This affects the shape and size of the BP cross-section in its folding with the transiting source. The parallactic angle q at which a source passes through the BP is given by the following formula:

$$\sin q = \cos\varphi \cdot \sin Az/\cos\delta, \quad (1)$$

where the azimuth $Az = 270°$, $\varphi = 43°49'53''$ is the geographic latitude of RATAN-600, and $\delta = 22°00'52''$ is the survey declination. Then

$$q = \arcsin(-\cos 43°.83/\cos 22°.0) = -48°.3\ (48°19'47''). \quad (2)$$

Despite its complexity and dependence on the survey height, the RATAN-600 BP has been well explored, including for the Western Sector (Majorova et al., 2023). Knowledge of the BP shape enables more accurate data processing with separation of off-axis sources passing through the input horns of the radiometers at different BP cross-sections.

The data processing system at RATAN-600 has undergone substantial evolution from the use of paper carriers to the development of a flexible data processing system for RATAN-600 under the Unix operating system employing

Table 1. Parameters of radiometers of the type 5 receiving and measuring complex.

λ, cm	f_0, GHz	Δf, GHz	ΔT, mK/s	T_n LNA, K	T_a, K	T_s, K	Radiometer type	Note
6.4	4.7	0.6 (0.15 × 4)	3.5	24–32	22	60	TP	3 radiometers, 12 channels

the standard FADPS package (Verkhodanov et al., 2005). This package satisfies all requirements for processing one-dimensional data that pass through the BP center. The data processing technique for sources passing outside the BP axis of the telescope was outlined in Bursov (2003). However, the processing of data associated with the angular passage of sources through the BP using the fixed antenna requires a comprehensive approach, described in this work. A technique and a corresponding software incorporating modules from the FADPS package have also been developed.

Thus, the aim of this work is to develop a technique for processing the survey carried out with the fixed antenna at one of the azimuths for sources passing through the BP at a parallactic angle to the horizon and to develop the corresponding software.

2 Antenna and radiometric complex

Observations at the RATAN-600 Western Sector (azimuth 270°) with the fixed antenna have been carried out since 2017. During each observation year, the fixed antenna is directed at a specified height for each individual survey. The present work is based on a survey conducted at the declination of the pulsar in the Crab Nebula ($\delta = +22°$, $H_0 = 32°48'47''$).

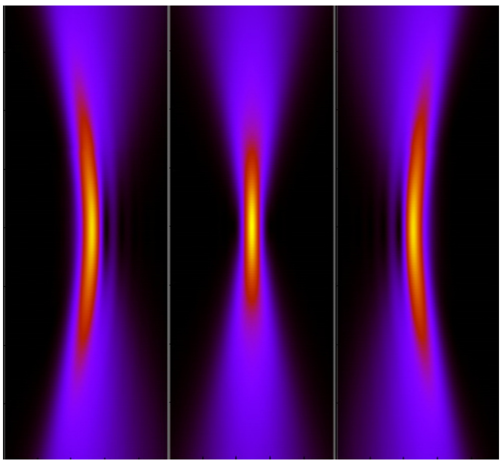

Fig. 1. Computed BPs for three input horns of radiometers with aberrations due to lateral offsets (±3′) at the declination of the Crab Nebula ($\delta = +22°$).

Sources pass through the BP with dH offset relative to the center, where $dH = H_0 - H_{\rm src}$. The greater the angular distance of the source from the center, the larger its half-power beam width and the lower the signal amplitude while preserving the integral (the product of amplitude and half-width), as seen on the computed BP images (Fig. 1) for each input horn of the radiometers. The images were constructed accounting for the computed aberrations of the offset horns.

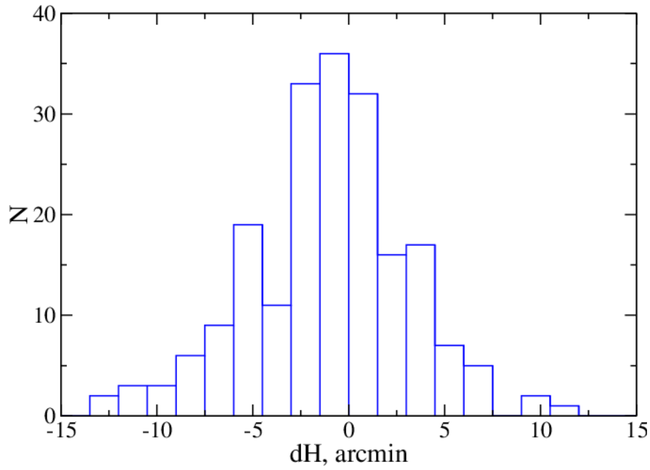

Fig. 2. Histogram of the distribution of source offsets relative to the BP center (in dH).

The BP calculations incorporated the specific characteristics of the radio telescope antenna system in this operating mode: the use of an oversized secondary mirror, asymmetric illumination of the primary mirror, and the arrangement of the primary feeds (horns) along the focal line of the secondary mirror (Korzhavin, 1977; Majorova, 2002). The distribution of sources in dH is shown in Fig. 2, which reveals a decline in the number of sources with increasing offset. This is associated with a decrease in sensitivity of the vertical BP in signal amplitude.

Consequently, for a survey area containing bright sources of $360° \cdot \cos(22°) \cdot 0.45° \approx 150^{\circ 2}$, their density is $205/24\text{h} <$ 10 sources per hour, or $205/150^{\circ 2} \sim 1$ source per square degree, which is negligible for confusion effects. Nevertheless, source blending occurred, but such cases were not taken into consideration.

To carry out continuum observations with RATAN-600, the new ER-DAS data acquisition and control system was employed. This is a measurement system intended to digitize and process radiometer signals and to transmit the results via Ethernet networks. The ER-DAS system has a low level of intrinsic noise and is free from $1/f$ noise. The radiometer type is a total-power radiometer with a wide reception bandwidth and a low coefficient of amplifier noise. On timescales up to 100 seconds, the sensitivity of such a radiometer is higher than that of a Dicke radiometer (Tsybulev et al., 2018).

Table 1 shows the principal characteristics of the radiometers used for observations. The following notation is adopted: λ – observing wavelength, f_0 – central observing frequency, Δf – received frequency bandwidth, ΔT – sensitivity at a time constant of 1 second, T_n LNA – noise temperature of the low-noise amplifier, T_a – antenna noise temperature at middle angles, T_s – noise temperature of the radio telescope – radiometer system, TP – total-power radiometer.

3 Data processing technique

In the first stage of data processing, records corrupted by atmospheric interference or instrument failures were filtered by dispersion. The remaining records in the radiometer channels were averaged according to the coupling coefficients. Hourly averaging of the records was then performed in a robust way based on the Hodges – Lehmann estimator (Hodges Jr., Lehmann, 1963). Detection and identification of bright objects with $S/N > 50$ in the averaged records were performed using source coordinates from the NVSS catalog, included in the CATS astrophysical catalog database (Verkhodanov et al., 1997). Source positions were computed using the software base of the ephemeris support for RATAN-600 (Korzhavin et al., 2012). The O−C shift (O – observed source positions, C – ephemerides) of sources relative to the fixed antenna due to precession of the Earth's axis depending on right ascension is shown in the top panel of Fig. 4.

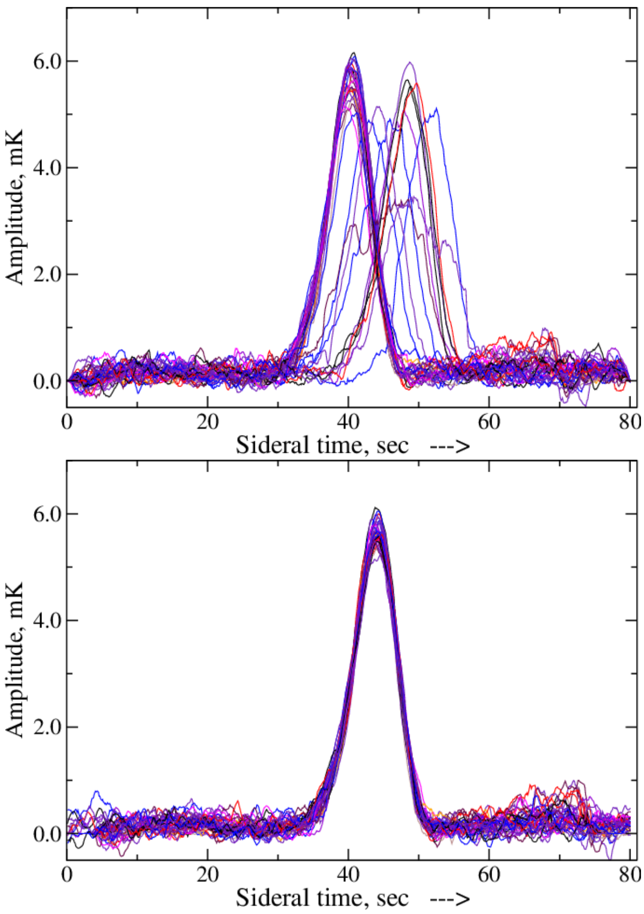

Fig. 3. Source NVSS 175915+215933. Top: initial interference-free data for the year of observations (values averaged over each 10-day interval). Bottom: data after correction for ephemeris, time and amplitude synchronization, with changes in the gain of radiometers taken into account.

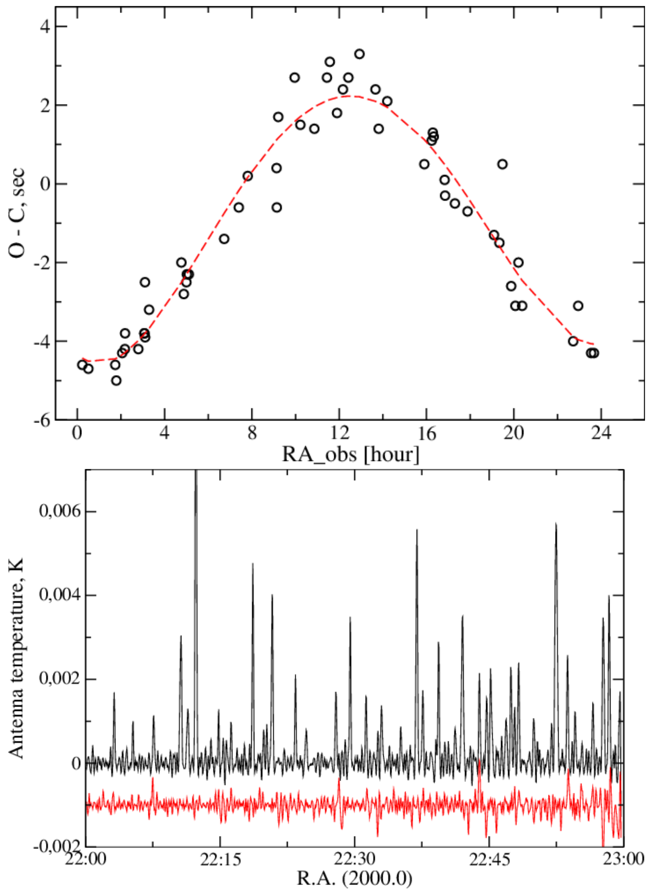

Fig. 4. Record averaging. Top: source position shifts due to precession depending on an hour angle. Bottom: example of signal accumulation for the half-sum (black) and half-difference (red) of records for R.A. = 22 h.

A precise binding with subsequent correction for records was carried out based on a sample of sources. The brightest sources were used for time synchronization, as well as sources with stable emission for amplitude correction. In the absence of radiometer calibration signals, amplitude correction was performed using the light curves of the Crab Nebula. Determination of source characteristics – apparent position, amplitude, and half-width determining their size – was carried out using the Gaussian analysis method. A software incorporating modules from the FADPS package was developed for this processing algorithm.

Figure 3 shows the source NVSS 175915+215933. The left panel demonstrates the interference-free records obtained over the year of observations; the right panel shows the data after correction for ephemeris, precise reference to time and amplitude, and after correction for temperature changes in the gain of radiometers.

During accumulation, records were hourly divided into two groups equal in quality. The half-sum – the mean of the two groups for each hour – contains both noise and signal. The half-difference contains only noise and negligible noise from the residual difference of sources (Fig. 4, bottom). For the calculation of the noise signal level dispersion, one can

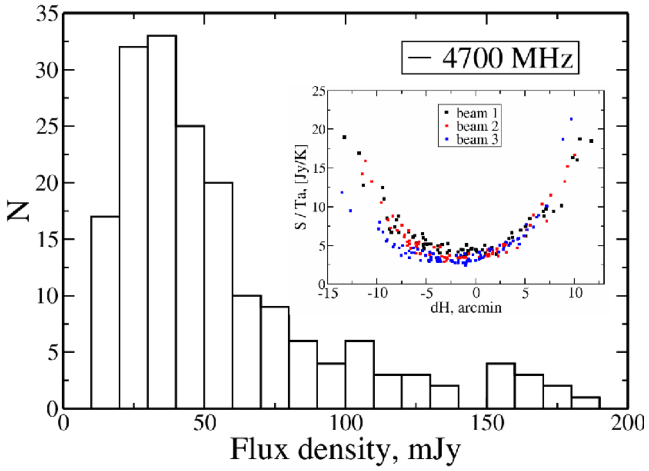

Fig. 5. Histogram of the flux density distribution for 205 bright survey sources at 4.7 GHz; the inset shows the calibration curves for the flux density.

write

$$\sigma^2 = \sigma^2_{(I+II)/2} - \sigma^2_{(I-II)/2}. \quad (3)$$

Thus, source signals in the averaged hourly records are estimated relative to records containing noise only.

Flux density determination is performed using a sample of the brightest survey sources ($S_{4.7} > 15$ mJy) with steep spectra and stable emission. Flux density values are determined from the approximation of radio spectra at 4.7 GHz. These are used to construct calibration curves: the ratio of the flux density of each source at the survey frequency ($S_{4.7}$) to its antenna temperature T_a, depending on the source offset from the BP center of each beam, $S_{4.7}/T_a \sim f(\Delta H)$. Figure 5 shows the histogram of the spectral flux density distribution for the 205 sources detected in the survey at 4.7 GHz. The inset shows the calibration curves for the flux density for three radiometers.

4 Conclusions

A data processing technique and a software have been developed for sky surveys conducted with the fixed antenna in azimuth at the RATAN-600 Western Sector since 2017 to the present. The technique was developed as a result of processing the 205 brightest ($S/N > 50$) survey sources at the declination of the pulsar in the Crab Nebula (Dec = 22°) at an azimuth of 270° at a frequency of 4.7 GHz. The technique accounts for aberrational distortions of the antenna BP, correction of records for changes in the gain of radiometers depending on ambient temperature and variation in the position of sources due to precession and nutation. The proposed processing method allows one to determine both the positions of detected sources with an accuracy of 1–2 seconds and flux densities with an accuracy of 5–10%.

On the basis of the developed technique, flux density was estimated for survey sources, radio spectra were explored, as well as time variation in the emission flux.

Acknowledgements. Observations with the SAO RAS telescopes are supported by the Ministry of Science and Higher Education of the Russian Federation. Instrumentation upgrades are being carried out within the framework of the national project “Science and Universities”.

This work was carried out within the framework of the SAO RAS state assignment approved by the Ministry of Science and Higher Education of the Russian Federation.

The authors are grateful to the referee whose constructive comments contributed to improving the paper.

References

Bursov N.N., 2003. Deep sky surveys at RATAN-600 (Phd thesis). Special Astrophysical Observatory of the Russian Academy of Sciences.

Bursov N., Trushkin S., Kudryashova A., et al., 2022. In A.M. Cherepashchuk, et al. (Eds.), Astronomy at the Epoch of Multimessenger Studies. pp. 354–355. doi:10.51194/VAK2021.2022.1.1.141.

Hodges Jr. J.L., Lehmann E.L., 1963. The Annals of Mathematical Statistics, vol. 34, no. 2, pp. 598–611.

Korzhavin A.N., 1977. Astrophys. Invest. (Bull. Spec. Astrophys. Obs.), vol. 8, pp. 53–70.

Korzhavin A.N., Lv́ov V.N., Tokhchukova S.K., Tsekmeister S.D., 2012. Astrophysical Bulletin, vol. 67, no. 2, pp. 225–229.

Majorova E., 2002. Bull. Spec. Astrophys. Obs., vol. 53, pp. 78–94.

Majorova E.K., Bursov N.N., Trushkin S.A., 2023. Astrophysical Bulletin, vol. 78, no. 3, pp. 429–442.

Pariiski I.N., Bursov N.N., Lipovka N.M., Soboleva N.S., Temirova A.V., 1991. Astron. Astrophys. Suppl. Ser., vol. 87, pp. 1–32.

Tsybulev P.G., Nizhelskii N.A., Dugin M.V., et al., 2018. Astrophysical Bulletin, vol. 73, no. 4, pp. 494–500.

Verkhodanov O.V., Trushkin S.A., Chernenkov V.N., 1997. Baltic Astronomy, vol. 6, pp. 275–278.

Verkhodanov O.V., Doroshkevich A.G., Naselsky P.D., et al., 2005. Bulletin of the Special Astrophysics Observatory, vol. 58, pp. 40–50.

Volvach A.E., Larionov M.G., 2008. Izv. Krymsk. Astrofiz. Observ., vol. 104, no. 5, pp. 78–84.